

Chapter 2

Quantum Crystals. The Search for Supersolidity

The present chapter will consist of the two main parts devoted correspondingly to bulk and surface phenomena in quantum crystals. In the first part of the chapter we will discuss a notion of quantum crystals and their distinction from ordinary classical crystals from the point of view of Lindemann criterion [1, 2] for crystal melting. We will also use de Boer parameter to describe the quantum crystals. Note that it measures the degree of quantumness or the ratio of kinetic delocalization energy of zero vibrations to the potential energy [3]. We will discuss Andreev, Lifshitz theory [4] for the hydrodynamics of superfluid quantum crystals and the flow of zero vacancies [5–7] as well as recent Andronikashvili type of rotating experiments of Chan et al. [8–13] on non-classical moment of inertia [14, 15] and the search of supersolidity in the crystals of ^4He [16–21]. We will provide a short review of the important experimental and theoretical articles on this fascinating subject [22–36] published during last several years by several groups in Moscow and by other groups in the West. We will discuss the overall pessimism of the community with respect to the possible discovery of supersolidity in [8–12] and provide the alternative explanations connected with the mass flow of defects (impurities, dislocations, two-level systems, thermal vacancies and so on) relative to the crystalline lattice in the non-perfect crystals of solid ^4He [36–38]. Very convincing results belong here to Rittner and Reppy who showed the disappearance of the supersolid fraction in rotating experiments after good annealing of the quantum crystal [36]. We will start the second part of the present chapter with the brief discussion of classical [39–42] and quantum roughening [43, 44] for different crystal surfaces of solid ^4He and present the estimates for roughening transition in the framework of Nozieres [39] theory of Berezinskii-Kosterlitz-Thouless type [45, 46] as well as mean-field arguments of Andreev and Parshin [47]. We will also briefly consider the two branches of surface waves on the mobile rough interface—the melting-crystallization waves (predicted and experimentally discovered in Kapitza Institute in Moscow [47–49]) and the more standard Rayleigh waves typical for the free surfaces of the crystals [5].

2.1 Quantum Crystals. Phase-Diagram. The Search for Supersolidity

In the introduction to the Landau Theory of Superfluidity in [Chap. 1](#) we presented the phase-diagram of ^4He (see [Fig. 1.1](#)) and briefly discuss it. The phase-diagram contains superfluid and normal liquid phases as well as gas and solid phases. Moreover there is no triple point where the liquid, solid and gas phases would coexist. For pressures $P > 26$ bar ^4He becomes solid. On the melting curve at low temperatures solid ^4He has hexagonal (hcp) structure. Between 1.46 and 1.76 K it has a cubic (bcc) structure. Note that there is a shallow minimum on the pressure versus temperature (P – T) curve for solid-superfluid phase-boundary at $T \sim (0.5\text{--}0.6)$ K (see [\[40\]](#) and [Fig. 1.1](#)). Close to the melting curve the density of a solid phase is very close to the density of a superfluid phase and thus $\frac{\Delta\rho}{\rho} \sim 0.1$, where $\Delta\rho = (\rho_s - \rho_L)$. It means that the interparticle distance (as well as other parameters) of solid ^4He are very close to superfluid ^4He . Moreover close to the minimum on the P – T curve the latent heat Q corresponding to liquid–solid phase-transition is small and thus first order phase-transition from superfluid to solid phase could be considered to be close with some degree of precaution to a second order phase transition. The only essential difference between liquid and solid phases is a translational invariance in solid phase connected with the elementary translations of the crystal lattice and the change of the short range order when we go from liquid to solid phase. This change is connected with an appearance of elementary cell in solid ^4He and thus with a shape energy a shape energy defined by a shear modulus (see [Chap. 1](#)). This “proximity” effect [\[50\]](#) between solid and superfluid phases was a main motivation to search for some type of quantumness in crystalline ^4He at low temperatures.

2.1.1 Lindemann and de Boer Parameters

Additional support for these ideas came from the estimates of Lindemann [\[1, 2\]](#) and de Boer [\[3\]](#) parameters for solid ^4He .

2.1.1.1 Lindemann Parameters in Solid ^4He

As we already mentioned in [Chap. 1](#), Lindemann parameter [\[1, 2\]](#) is essential for melting of the crystal. It is the ratio of the root mean square of the displacement of atoms to the interatomic distance d :

$$\gamma_L \sim \frac{\sqrt{\langle \bar{u}^2 \rangle}}{d}. \quad (2.1.1)$$

The classical solid will melt if the Lindemann's parameter exceeds the critical value of the order of 0.1 in 3D. However, the X-ray measurement of Debye-Waller factor of solid ^4He at $T \sim 0.7$ K and near melting curve shows this ratio to be 0.262 [51]. Thus, γ_L in ^4He strongly exceeds γ_L in classical crystal and hence the solid ^4He can be named a Quantum crystal.

According to Andreev, Lifshitz considerations [4] a solid ^4He also possesses a large de Boer parameter.

2.1.1.2 de Boer Parameter for Solid ^4He

de Boer parameter Λ measures the ratio of kinetic delocalization energy and potential energy of the system:

$$\Lambda = \left(\frac{E_{kin}}{E_{pot}} \right)^{1/2}, \quad (2.1.2)$$

where total energy of the system $E_{tot} = E_{kin} + E_{pot}$. In solid ^4He the potential energy is connected with the standard 6–12 potential with hard-core repulsion and van der Waals attractive tail:

$$U(r) = 4\varepsilon \left[\left(\frac{d}{r} \right)^{12} - \left(\frac{d}{r} \right)^6 \right], \quad (2.1.3)$$

where ε is a characteristic energy of the two atom interaction and d is the inter-particle distance. Thus E_{pot} in (2.1.2) is of the order of ε close to the minimum (see Fig. 2.1.) where $r \sim d$. Correspondingly kinetic energy or zero-vibrations is given by:

$$E_{kin} \sim \frac{\hbar^2}{m\langle r^2 \rangle} \sim \frac{\hbar^2}{md^2}, \quad (2.1.4)$$

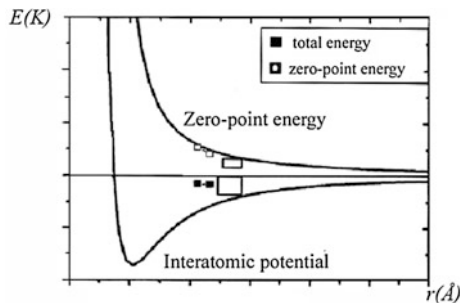
where m is a mass of ^4He atom. Hence:

$$\Lambda \sim \frac{\hbar}{d} \frac{1}{\sqrt{m\varepsilon}}. \quad (2.1.5)$$

On Fig. 2.1 we present interatomic potential and zero-point energy in solid ^4He as the functions of the distance r between the atoms.

In ordinary crystals de Boer parameter Λ determined by Eq. (2.1.5) is small. It becomes larger for inert gases. For instance $\Lambda = 0.6$ for Ne. However, for ^4He $\Lambda = 2.7$ is large (it is even larger for ^3He crystals $\Lambda = 3.1$ since the atomic mass m_3 is smaller than m_4). For $\Lambda > 1$ it means that the kinetic energy prevails over potential energy and we have the conditions for the delocalization of the atoms (for the large zero-vibration energy). In principal the number of atoms in such crystal should not necessary coincide with the number of the lattice cites. Moreover the

Fig. 2.1 Interatomic potential $U(r)$ and zero-point energy $E_{kin} = \frac{\hbar^2}{2md^2}$ in solid ^4He as the functions of the distance r between the atoms [8–13]



motion of the atoms (more precisely of the elementary excitations such as vacancies and defectons see [4]) should resemble the motion in ideal liquid i.e. should be without binding to the equilibrium position of the atom in the lattice. Thus it is appealing to describe such a system in analogy with liquid ^4He by a macroscopic Ψ -function of Jastrow type (see the papers by Chester and Reatto [17, 18]). The mutual permutations of the atoms in such a crystal could lead to the delocalization, or in the other words to the motion of vacancies in crystal (see Yang [19–21]).

2.1.1.3 Formal Theoretical Remark on off Diagonal Long Range Order (ODLRO) and Superfluidity

Note that Penrose and Onsager [19–21] emphasized that in a perfect solid each atom is localized at a specific lattice site and only lattice translational symmetry is present. Thus there is no Bose–Einstein condensation (BEC) [52] at $T = 0$ (when the thermal vacancies are absent and thus there is no band motion in the crystal). Moreover, according to Yang, the Off Diagonal Long Range Order (ODLRO), or superfluidity, which is directly related to Bose–Einstein condensation [53], may occur in a solid phase only if the particles are delocalized. In other words to have superfluidity in Quantum crystals we should have according to Matsuda and Tsuneto [16] the coexistence of DLRO (diagonal long range order) connected with translational symmetry and ODLRO, connected with superfluidity in the crystals.

These considerations are often used nowadays especially when the theorists investigate with respect to superfluidity (or supersolidity) the Bosonic models on the lattice [27–31]. More specifically they often consider Bose-Hubbard model or extended Bose-Hubbard model with short-range repulsion between bosons on one site and additional repulsion between them on the neighboring sites of the lattice (see Chap. 5 for more details). The main goal here is to find the region of parameters on the phase-diagram where a new phase with a superstructure (with an incommensurate density wave) can be stabilized on top of a crystalline lattice. This additional superstructure or superlattice (or density wave) will just correspond to ODLRO, while the initial lattice—to a standard translational long range order (DLRO). Thus such a new phase can be considered with some degree of precaution as a supersolid phase.

Note that these arguments are supported by the old idea to increase the pressure and thus to reduce the roton gap Δ to zero near the melting curve (see Fig. 1.2 for the spectrum of elementary excitations in the superfluid ^4He) and thus to create a superstructure or a superlattice with a period proportional to $1/p_0$ (where $\varepsilon(p_0) = \Delta$ for roton's minimum).

Note also that thermodynamics of an incommensurate quantum crystal was considered recently by Anderson, Brinkman and Huse [22, 23]. The authors of [22, 23] derived an effective Ginzburg–Landau (GL) functional for the incommensurate case when the number of vacancies (N_{vac}) does not coincide with the number of the interstitials (N_{interst}). The GL-functional is constructed in terms of the parameter of incommensurability δ which measures the difference between the ratio of $\frac{N_{\text{vac}}}{N_{\text{sites}}}$ at finite temperature and at temperature zero: $\delta = \frac{N_{\text{vac}}(T)}{N_{\text{sites}}} - \frac{N_{\text{vac}}(T=0)}{N_{\text{sites}}}$.

The vacancies and interstitials according to Anderson et al. are in strongly-correlated state and provide a small contribution to the entropy of the incommensurate crystal $\Delta S_{\text{cryst}} = \beta T^7$ [22]. The main contribution to the entropy is still due to phonons $\Delta S_{\text{cryst}} = \beta T^3$. In the next article [23] Anderson also proposed a model wave-function for a superfluid solid which accounts for the vacancy component [51] and Gutzwiller constraint [81]. The constraint prohibits the double occupancy of one site in quantum Bose solid.

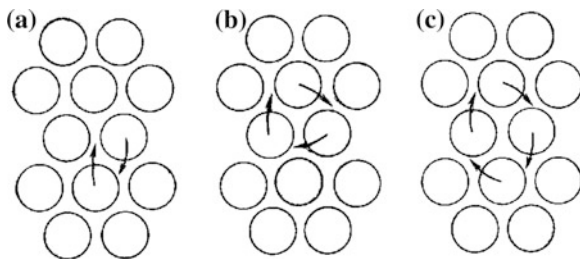
2.1.1.4 Quantum Permutations

In the absence of vacancies the permutations between particles are complicated in the perfect quantum crystal by large short-range Hubbard (or contact) repulsion between them (see Fig. 2.2).

2.1.2 Flow of Zero Vacancies. Andreev-Lifshitz Theory

However, usually there are vacancies, defects and impurities in the quantum crystals which make the permutations easier.

Fig. 2.2 Quantum permutations of two (a), three (b), and four (c) particles in a perfect quantum crystal without defects (from review-article of Andreev [43])



2.1.2.1 Vacancies, Defectons and Impuritons

In other words in quantum crystals besides a standard phonon branch of the elementary excitations should be an additional branch with a band character of motion. The most difficult logical point here is that the number of atoms can be different from the number of lattice sites in the quantum crystal. To realize this idea we need vacancies, dislocations, interstitials or other defects in the crystalline lattice. Another possibility to realize this scenario is to consider the system of impurities (^3He for example) in the crystalline matrix of ^4He . In this case the band character of impurity atoms (impuritons) leads to the phenomena of quantum diffusion (Andreev and Lifshitz [4], Y. Kagan and Maksimov [54–57]). Note that in ordinary crystals the spectrum of vacancies has a large energy gap and so their number and their contribution to specific heat are exponentially small. Andreev and Lifshitz assumed that in quantum crystal of ^4He the number of vacancies is of the order of 1 per site that is there are *zero vacancies* in the system. In definite conditions then (in particular in the absence of Mott–Hubbard localization—see Chap. 4, 5, 9 for more details) the vacancies could Bose-condense [52] and all the crystal will undergo the transition to the superfluid state. On the macroscopical language this state will be described by the many component superfluid hydrodynamics similar to Landau hydrodynamics [58] for superfluid liquid helium which was detailly considered in Chap. 1. To be more precise the hydrodynamics of a supersolid is even a bit closer to the hydrodynamics of rotating superfluid in a presence of the vortex lattice since it also contains three independent velocities.

One of them is \vec{v}_s —the velocity for the superfluid motion of zero vacancies (or other zero quantum defects). Another one \vec{u} stands for the lattice velocity. The third one \vec{v}_n is governed by the normal motion of elementary excitations such as thermal vacancies and phonons. Note that the two relative velocities $\vec{w}_1 = \vec{v}_s - \vec{u}$ and $\vec{w}_2 = \vec{v}_n - \vec{u}$ are nonzero in our case. Correspondingly besides the standard transverse and longitudinal sound in the phonon subsystem, we have an additional sound mode in the subsystem of vacancies (defectons) in a supersolid. The last mode a bit resembles the second sound in a superfluid liquid ^4He but does not exactly coincide with a second sound since a fraction of vacancies is superfluid. Nevertheless in analogy with a second sound the phase velocity of this mode depends upon the ratio ρ_n/ρ_s between the densities of thermal and superfluid vacancies. Note that since at $T = 0$ there is a finite difference $\Delta\rho/\rho \sim 0.1$ between the densities of solid and liquid phase we can expect the same amount of spatial disorder (or 10 % of surface vacancies) on the phase-interface between quantum crystal of ^4He and quantum superfluid He-II (see the next chapter). If we can organize the diffusive flow [80] of vacancies from the surface to the bulk of the crystal, we can probably create the sufficient amount of zero vacancies in the bulk solid ^4He and thus promote non-equilibrium superfluidity. If, vice versa, we believe that there is a lot of equilibrium zero vacancies in the bulk, than we can create the diffusive flow of vacancies in the opposite direction—from the bulk to the surface and in this way to measure the spatial distribution of vacancies (or defectons) and the gradients of their density.

2.1.2.2 Zero Vacancies. Theoretical Background

Andreev and Lifshitz assumed the following bare spectrum of vacancies in solid ^4He :

$$\varepsilon(p) = \varepsilon_0 + \frac{p^2}{2M}, \quad (2.1.6)$$

where $\varepsilon_0 < 0$ is negative at low temperatures and M is an effective mass of vacancion (which in principle can be different from the mass of ^4He atom m_4). In solid ^4He vacancies are bosons, as well as ^4He atoms themselves. In general we have weakly non-ideal low-density Bogoliubov Bose-gas with repulsive interaction between vacancies [53]. In this case the chemical potential μ is negative for low density of vacancies $n_V d^3 \ll 1$. Indeed in the Hartee-Fock approximation the chemical potential reads [4, 43]:

$$\mu = -|\varepsilon_0| + \frac{4\pi\hbar^2}{M} f_0 n_V < 0, \quad (2.1.7)$$

where $f_0 > 0$ is repulsive scattering amplitude and $\frac{4\pi\hbar^2}{M} f_0$ is pseudo potential for the vacancies interaction (see Chap. 6). Of course, in this situation the vacancies will be Bose-condensed at the temperature given by Einstein formula $T_C^{BEC} \sim \frac{3.31 n_V^{2/3}}{M}$ [52]. Moreover after diagonalization of the Bogoliubov Hamiltonian for vacancies (after Bogoliubov u-v transformation [53]) their transformed spectrum will read:

$$E(p) = \sqrt{c^2 p^2 + \left(\frac{p^2}{2M}\right)^2}. \quad (2.1.8)$$

It will become linear at small momenta $E(p) = cp$, where

$$c^2 = \frac{4\pi\hbar^2}{M^2} f_0 n_V \quad (2.1.9)$$

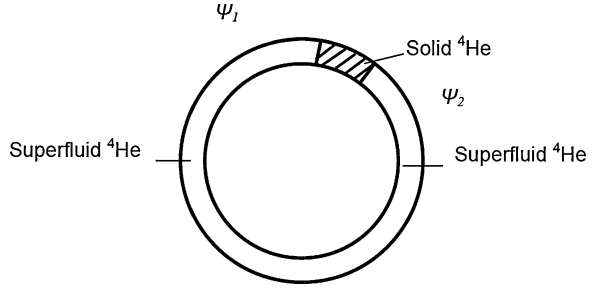
is a sound velocity squared (see Chap. 6 for more details). Thus the Bogoliubov spectrum of vacancions (2.1.8) will satisfy Landau criterion for superfluidity (see Chap. 1).

2.1.2.3 Zero Vacancies. Experimental Search

The attempts to find experimentally zero vacancies were based on three main ideas:

1. To perform an analog of Josephson experiment in a ring where a thin peace of solid ^4He serves as a cork to superfluid ^4He (see Fig. 2.3) and to find the manifestation of the macroscopic wave-function Ψ which penetrates in the solid and connects left and right branches of the superfluid ^4He via the small cork [59] of atomic size.

Fig. 2.3 The principal scheme of the gedanken Josephson-type of experiment in a ring where a piece of solid ^4He serves as a cork to superfluid ^4He

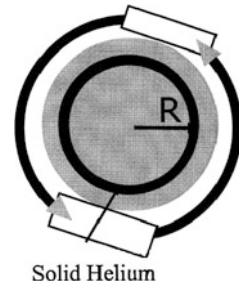


2. To measure the low-temperature specific heat in solid ^4He [6, 7, 13, 60, 61] and to subtract a phonon contribution proportional to T^3 thus finding (if it exists) the contribution of zero-vacancies $C_V \sim \exp\{|\varepsilon_0|/T\}$. Another possibility is to measure the temperature dependence of the melting pressure $P(T)$ at low temperatures and to subtract T^4 contribution due to phonons (Parshin et al. [38]).
3. To perform an analog of Andronikashvili experiment [14] with rotation of solid ^4He and to extract a non-zero superfluid fraction $(1 - \rho_n/\rho) = \rho_s/\rho$ from the non-classical moment of inertia (Leggett's idea [15], experiments of Chan et al. [8–12]) if supersolidity exists.

Unfortunately until now numerous measurements do not confirm the existence of zero vacancies. Namely in NMR, X-ray and acoustic measurements experimentalists observe only the contribution of thermo-activated vacancies. In the same time in the measurements of specific heat and heat conductance as well as of the temperature dependence of the melting pressure all the results can be explained only by phonon contribution without vacancies at all. If there is some small vacancy contribution in these experiments, it is connected with bosonic (and not Boltzman) vacancies with a broad band and a complicated spectrum. Finally in the experiments on thermal expansion in solid ^4He at high temperatures the researchers observe Anderson's type of the corrections to the specific heat $\delta C_V \sim bT^7$. These corrections can be possibly explained by some degree of incommensurability according to Anderson et al. [22, 23], but not by the thermoactivative vacancies.

Thus the problem of the experimental search of zero vacancies is opened for future investigations in different quantum solid systems with large Lindemann and de Boer parameters. Maybe the better conditions for supersolidity can be experimentally achieved in excitonic systems (Balatsky et al. [24–26]) and in ultracold Bose-gases on optical lattices where it is easier experimentally to tune the parameters of the system.

Fig. 2.4 The principal scheme of the gedanken Leggett's type of experiment to measure the non-classical rotation inertia in rotating solid ^4He [15]



2.1.2.4 Leggett's Idea

The ideal method to detect superflow according to Leggett [15] would be to subject solid ^4He to undergo dc or ac rotation and to look (in similarity with Andronikashvili experiments in superfluid ^4He) for the evidence of Non-Classical Rotation Inertia (NCRI—see Chap. 1).

Quantum exchange of particles arranged in an annulus under rotation leads to a measured moment of inertia that is smaller than the classical value (see Fig. 2.4 and [8–13, 61]). Namely the moment of inertia $I(T) = I_{\text{classic}}(1 - f_s(T))$, where $f_s(T) = \rho_s/\rho$ is the supersolid fraction.

2.1.3 Chan Experiments with Rotating Cryostat. The Search for Supersolidity in Solid ^4He

Recently an attempt to realize the Leggett's idea was made by the group of Chan [8–13, 61] in Penn State University, USA (see Fig. 1.7 in Chap. 1 for the principal scheme of the experimental setup used by Chan's group). In the first paper Kim and Chan filled the pores of Vycor glass (of aerogel, see Chap. 3) with solid ^4He and studied the rotation of this solid system. They observed that effective moment of inertia was smaller than the total one at low temperatures $T < 0.125$ K. The authors interpreted their result as a transition of solid ^4He in pores in a superfluid state. This result produced a huge interest in the low temperature community and casts doubts connected with the side effect of porous medium. Trying to reduce the skepticism Kim and Chan published two more articles where they have studied the moment of inertia of solid ^4He in the absence of aerogel and at small concentration of ^3He impurities (clean situation). They worked close to the melting line on the phase diagram of ^4He and carefully studied thermodynamics close to its minimum at $T \sim (0.5 \div 0.6)$ K where nontrivial quantum effects cannot be excluded in principle. They claimed that $\rho_s \leq 0.01 \rho$ in these experiments (1 % of superfluid fraction). However, scientific community again was not convinced even by these results. Rittner and Reppy [36] challenging Chan's results showed experimentally that, when all the defects like grain boundaries, dislocations etc. are carefully

annealed and when we have a very pure crystal, the effect of non-classical moment of inertia disappears. So now the most part of the low temperature community (see papers by Andreev [33–35], Balatsky et al. [24–26], Prokof'ev et al. [27–31], Parshin et al. [38], Balibar et al. [32]) does not believe in the real supersolidity but more in some glassy state with a superflow of defects (grain boundaries etc.) relative to the lattice [59]. Note that in glasses (like SiO_2 for example) the number of equivalent sites under deformation is larger than the number of atoms. Therefore two types of motion are possible in a glassy state: oscillations near the equilibrium positions (analogous to phonon modes in regular solids) and sudden “jumps” of diffusive types from initial state to the neighboring equivalent positions.

Equivalently upon deformation of a quantum crystal there arises a self-consistent motion of lattice sites and a flow of defectons, accompanied by a transport of mass. According to the recent discussion of Andreev-Lifshitz theory in Kavli Institute [62] with some degree of precaution we can speak about possible “superplasticity” of a quantum crystal.

The important recent observation should be mentioned here in this context, namely the increase of a shear modulus in ^4He crystal at low temperatures $T \sim 0.1$ K instead of a decrease typical for superfluid or “superplastic” quantum crystal. The increase of the shear modulus K can produce a drop in the resonant period $T = 2\pi\sqrt{I/K}$ without a decrease of the moment of inertia I [83, 84], and thus without a real supersolidity. In their recent experiments [83] Kim and Chan confirmed the increase of the shear modulus at low temperatures due to solidification of one ^4He layer and the absence of the superfluid fraction. These results according to Kim and Chan [83] prove the absence of supersolidity in solid helium in porous vycor glass. Another interesting aspect to be mentioned is an idea of Y. Kagan [63] about the possibility of the choc-ice model for the explanation of the rotating experiments of Chan et al. Namely due to a small difference of densities between solid and liquid phases it could be probably easier to have a surface melting of the crystal instead of melting in the bulk. Then it is possible to create a surface layer of superfluid ^4He between the crystal and the walls of rotating experimental container similar to the surface melting of ice-cream in a glass. This melted surface layer becomes superfluid and can in principle explain the difference between a measured moment of inertia connected with rotation and a total moment of inertia of a solid in the absence of aerogel.

2.2 The Surface Physics of Quantum Crystals. Atomically Smooth and Atomically Rough Surfaces

We proceed now to the second part of the chapter where we will concentrate mainly on the surface physics for the different phase-interfaces of the solid ^4He in contact with superfluid helium. It is also a subject of a hot debate today especially concerning the problem of quantum and classical roughening and the correlation between microscopic models of roughening and macroscopic hydrodynamics on

atomically (or even quantum) rough surfaces where the spectrum of weakly damped melting-crystallization waves $\omega \sim k^{3/2}$ was measured. These measurements were performed not only for relatively high (roton) temperatures $T \sim (0.7 \div 1.2)$ K but also for much lower (phonon) temperatures $T \sim (0.3 \div 0.6)$ K. In this section we will try to present a now-a-day understanding of the problem and emphasize the unresolved questions which still, according to our point of view, do not allow to construct the coherent microscopic physical picture of a mobile phase-interface between quantum solid and quantum liquid.

2.2.1 The Concept of the Mobile Rough Interface Between Solid ^4He and Superfluid He-II

As we understood in the Introduction to Sect. 2.1, the ^4He atoms in quantum crystals have large zero-vibration energy of quantum oscillations and can be considered as delocalized or almost delocalized quasiparticles. The atoms of superfluid helium are also delocalized and participate (even in the absence of a drift flow) in a coherent oscillating motion of the Bose-condensate. Thus with some degree of precaution it is appealing to talk about the joint macroscopic Ψ -function which connects solid and liquid subsystems via a coherent phase-interface (see [50]). In fact the situation is more complicated especially at zero temperature (at $T = 0$) (see [40]).

In the series of the pioneering papers Castaing and Nozieres [64], Andreev and Parshin [47], Marchenko and Parshin [65] developed the ideas of *delocalized atomically* (or even quantum) *rough* state of the interface (see Fig. 2.5) and the

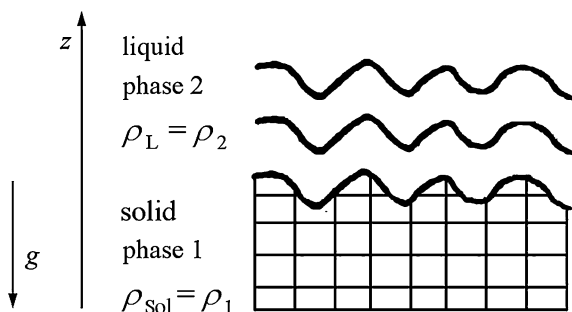


Fig. 2.5 The qualitative picture of the surface hydrodynamic waves on the mobile rough interface between solid and superfluid ^4He . At low frequencies these waves are melting-crystallization waves (see the next section). For these waves we can introduce $z = \zeta + u_s$ for a total displacement of the surface point from equilibrium position (see explanation below). \vec{g} is gravitational acceleration, ρ_{sol} , ρ_L are the densities of solid and liquid phase

roughening transition (Nozieres [39], Andreev [43]) between atomically rough (or quantum rough) and atomically smooth states of the interface.

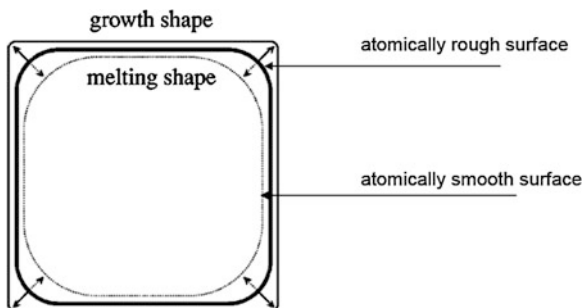
2.2.2 Growth and Melting Shape of a Crystal

On Fig. 2.6 we present growth and melting shapes of ^4He crystal following a nice review-article of Balibar et al. [40]. We can see the rectangular parts on Fig. 2.6 corresponding to atomically smooth surfaces (or facets) and rounded corners corresponding to atomically rough surfaces. An important observation is that facets grow and melt more slowly than atomically rough rounded corners. Thus atomically rough interfaces are more mobile. Remind that a crystal grows from a liquid phase when we increase a pressure a little bit (create an overpressure) working near the melting curve. Note also that the classical crystals at low temperatures always have characteristic faceting and melting-crystallization processes on them are very slow (see review-article of Chernov [66] for example). The quantum crystals in contrast to the classical ones have extended atomically rough regions (see Fig. 2.6) with rapid melting-crystallization processes on the rough surfaces.

2.2.3 Melting-Crystallization Waves and Phase Equilibrium on the Mobile Rough Surface

The atomically rough surface state together with the small difference between the densities of bulk solid and superfluid phases $\Delta\rho/\rho \sim 0.1$ and between zero-vibration energies of liquid and solid phases promote rapid and practically dissipationless character of melting-crystallization processes on the phase boundary. In fact it is possible to incorporate the atom from the liquid rather rapidly and over a small potential barrier in the surface atomic row in the crystal. The rapidness and practically dissipationless character of melting-crystallization waves on the rough surface [47–49, 76, 77, 82] in macroscopic language can be expressed in the

Fig. 2.6 Growth and melting shapes of a crystal from [40]. Facets grow and melt more slowly than atomically rough rounded corners



condition of the thermodynamic equilibrium on the boundary $\mu_1 = \mu_2$ for chemical potentials of solid and liquid phases (see Fig. 2.5). Together with the standard boundary condition for the mechanical equilibrium $P_1 = P_2$ for the pressures (see [5]) and thermodynamic identities at $T = 0$ $\delta P_1 = \rho_1 \delta \mu_1$ and $\delta P_2 = \rho_2 \delta \mu_2$ for small pressure deviations, we can use the equation $\delta \mu_1 = \delta \mu_2$ for the deviations of the chemical potentials from equilibrium to get:

$$(\rho_1 - \rho_2) \delta \mu_2 = 0. \quad (2.2.1)$$

Hence $\delta \mu_2 = 0$ and $\delta P_2 = 0$ for the liquid phase, where δP_2 is the difference between local pressure in the liquid and the equilibrium one $P_0 = 26$ bar. Thus the atomically rough interface between solid and superfluid ^4He becomes equivalent to the free interface between liquid and vacuum. Note that in more rigorous considerations there are surface (capillary) terms [58] of the Laplace type in the right-hand side of (2.2.1) (see the next section). As a result the melting-crystallization waves on the rough surface resemble according to Andreev and Parshin [47] the standard capillary waves on the free surface of the liquid [58]. These waves are sometimes called riplons and for liquid-vacuum interface have the spectrum $\omega^2 \sim (\alpha/\rho) k_{\parallel}^3$, where α is the surface tension coefficient and k_{\parallel} is a projection of the wave-vector parallel to the free surface (see also Chaps. 3 and 15). Correspondingly for the mobile rough interface between solid and superfluid ^4He $\omega^2 \sim \frac{\alpha \rho}{(\Delta \rho)^2} k_{\parallel}^3$ where $\rho/(\Delta \rho)^2$ is a specific density factor for this interface. The spectrum and damping of melting-crystallization waves will be derived more rigorously from the linearization of the equations of the surface hydrodynamics in the Chap. 3. Note that for melting-crystallization waves the growth velocity $V_b = \dot{\zeta}$ of the boundary does not coincide with the lattice velocity \dot{u}_z (see Fig. 2.5). Note also that more rigorously in the spectrum of melting-crystallization waves instead of a surface tension coefficient α enters the surface rigidity $\tilde{\alpha}$ (see Chap. 3).

2.2.4 Rayleigh Waves on Rough and Smooth Surfaces

Another branch of the surface waves which usually corresponds to higher frequencies on mobile solid—superfluid interface is a more standard one. In this branch we neglect melting-crystallization processes and get for the rough surface:

$$\delta P_1 = \delta \sigma_{zz} = 0; \delta \sigma_{z\alpha} = 0; \rho_2 \delta \mu_2 = \delta P_2 = 0 \quad (2.2.2)$$

for the oscillating parts of the pressures P_1 and P_2 and the stress-tensor components σ_{zz} and $\sigma_{z\alpha}$, $\alpha = \{x, y\}$ (note that z-axis corresponds to the normal to the surface).

In other words while for melting-crystallization waves the total growth velocity of the boundary $V_b = \dot{\zeta} + \dot{u}_z \approx \dot{\zeta}$ (and correspondingly the lattice velocity $\dot{u}_z \approx 0$), for Rayleigh waves we have vice a versa $V_b \approx \dot{u}_z$ and $\dot{\zeta} = 0$ for the recrystallization rate. Hence the rough interface between solid and liquid becomes equivalent at high frequencies to the interface between solid and vacuum. On this interface

the standard Rayleigh waves can propagate (see Landau, Lifshitz Elasticity Theory [5]) in similarity with the surface of the crystal with vacuum. The spectrum of the Rayleigh waves is linear:

$$\omega = \eta c_t k_{||}, \quad (2.2.3)$$

where c_t is transverse sound velocity in solid (see also Chap. 1) and in isotropic approximation the coefficient $\eta = \eta(c_t/c_l)$ depends upon the ratio between transverse (c_t) and longitudinal (c_l) sound velocities in solid phase. In solid ^4He $\eta \sim 0.8 \div 0.9$. Note that as we discussed there are different interfaces of solid ^4He . Their character (atomically smooth or atomically rough) depends on their orientation to the main crystallographic axis of the crystal (we consider mostly hexagonal hcp structure of the ^4He crystal). Some of the interfaces are atomically rough at low temperatures. They are rapidly growing mobile surfaces. On these surfaces we have two branches of the surface waves: melting-crystallization waves at low frequencies and Rayleigh waves at higher frequencies (see the more precise derivations in the next chapter).

The other interfaces grow much slower. They are atomically smooth and obey more standard laws of growth. They have characteristic faceting (see Fig. 2.7) and only Rayleigh waves (more precisely Rayleigh-Stonely waves) propagate on their surface in the linear regime. The spectrum of melting-crystallization waves on them is strongly modified and becomes non-linear (amplitude-dependent) see Parshin and Gusev [67].

2.2.5 Roughening Transition

There are two main competing approaches to the roughening transition in solid ^4He which belong to Nozieres [39] and Andreev and Parshin [47] respectively (see also quantum models of Iordanskii and Korshunov [44]). Note that the roughening transition takes place, generally speaking, in the 2D gas of steps and kinks on the surface. Thus, steps and kinks serve as elementary excitations in surface science which define the kinetics and thermodynamics of surface growth as well as the roughening transition from atomically smooth to atomically rough state of the surface. Let us remind that a step is an additional row of atoms which joins already exciting terrace for a flat part of the surface (see Fig. 2.8). It is important to emphasize that besides straight “bare” steps there are also steps with kinks, where the kink is an additional atom (adatom) on a straight “bare” step (see Fig. 2.8).

According to Andreev and Parshin there are surfaces which can be in atomically (or quantum) rough state till very low temperatures due to delocalization of quantum kinks on the steps. In this case Andreev and Parshin assume that the energy of a step with kinks reads (see [47]):

$$\beta = \beta_0 + d \left(-\frac{\Delta}{2} + \varepsilon \right), \quad (2.2.4)$$

Fig. 2.7 Faceting of ^4He crystals from Balibar, Guthmann and Rolley [71]. As temperature goes down, more and more facets appear at the surface of ^4He crystals. From *top to bottom*, the temperature is successively 1.4, 1, 0.4, and 0.1 K. When we decrease the temperature more surfaces become atomically smooth

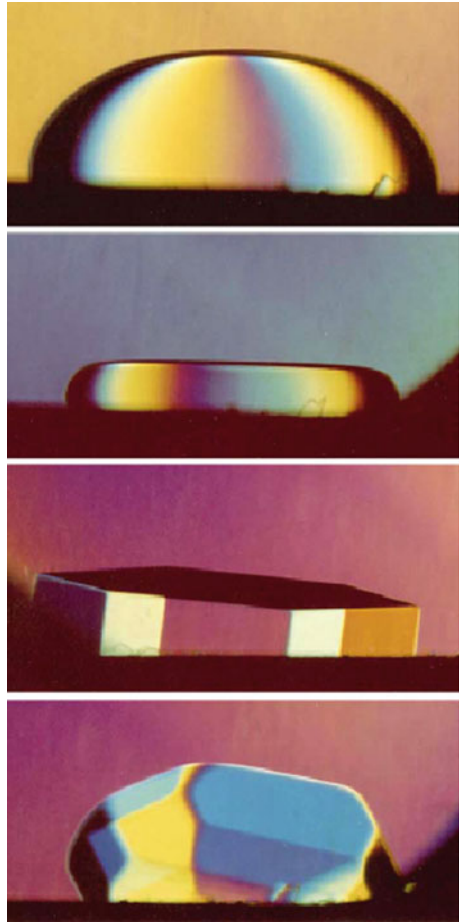
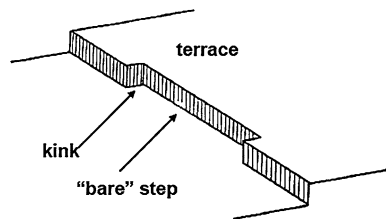


Fig. 2.8 A step with kinks on the growing surface (from [43])



where β_0 is an energy of a straight “bare” step without kinks, d is intersite distance, Δ is the bandwidth for delocalized kinks and ε is the kinks quasiparticle energy counted from the bottom of the band (from $-\frac{\Delta}{2}$). For highly delocalized ensemble of kinks the second term in the r.h.s of (2.2.4) can coincide by the order of magnitude with the first one $(\frac{\Delta}{2} - \varepsilon) \sim \frac{\beta_0}{d}$.

It means that the kinks quasiparticle energy coincides by the order of magnitude with a step energy per unit length. Correspondingly β in (2.2.4) can tend to zero or even becomes negative for the bottom of the band for zero vacancies. So we can have a quantum rough state with no steps (or highly delocalized “zero-point” steps) and with only rounded parts of the surface already at low temperatures. At some finite temperature T_R Andreev and Parshin predicted a mean-field (second order) phase transition from quantum rough state to a classical rough state. Nozieres [39] has quite different point of view. According to Nozieres [39] (see also [40] for an extended review) the roughening transition between low temperature atomically smooth phase and high-temperature atomically rough phase takes place at a finite temperature T_R and is governed by Berezinskii—Kosterlitz—Thouless (BKT)—type [45, 46] of the transition in 2D gas of steps. In the approach of Nozieres for high temperatures $T > T_R$ the steps are delocalized and highly fluctuating and thus we can put a step energy $\beta = 0$ for $T > T_R$. In the same time for $T < T_R$ the macroscopically large steps are formed. As a result the typical size of the terrace on Fig. 2.8 (effectively the coherence length) should diverge and all the surface becomes flat. Thus, we are in atomically smooth state at $T < T_R$. The atomically smooth surface is faceted and very slowly growing. Its growth velocity $V_b \rightarrow 0$. Note that the step energy β in Nozieres theory plays a role of a superfluid density ρ_s in BKT-theory for 2D ^4He -films. Thus, it should be a finite jump in β at T_R . Correspondingly we can estimate the roughening transition temperature T_R in the same way as T_{BKT} for a 2D superfluid film. Namely:

$$T_R \sim d\beta(T_R), \quad (2.2.5)$$

where βd is a step energy calculated for one atom at $T = T_R$.

In surface science it is convenient to introduce also the angular dependent surface energy $\alpha(\varphi)$. For the atomically smooth surface with steps of the atomic height the surface energy reads for small angles $\varphi \ll 1$ (see Fig. 2.9):

$$\alpha(\varphi) = \alpha_0 + \frac{\beta}{d}|\varphi| + \gamma|\varphi|^3, \quad (2.2.6)$$

where $\frac{\beta}{d}$ is a step energy of unit height, γ is an interaction energy between the steps.

Note that in solid ^4He $\alpha_0 \sim 0.127 \frac{\text{erg}}{\text{cm}^2}$, $\frac{\beta}{d} \sim 1.3 \cdot 10^{-2} \frac{\text{erg}}{\text{cm}^2}$, $d \sim 3 \text{ \AA}$. The coefficient γ is a subject of a debate and is different in the estimates of different groups.

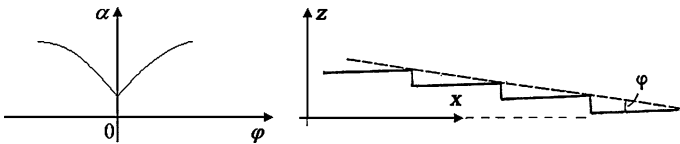


Fig. 2.9 The angular dependence of the surface energy $\alpha(\varphi)$ for $\varphi \ll 1$ for the surface with steps of the atomic height, d is interatomic distance

Note also that according to Landau [42] the derivative $\frac{\partial \alpha}{\partial \phi}$ has a finite jump $\frac{\beta}{d}$ at $\phi = 0$ for atomically smooth surfaces.

Another important and widely used quantity is the so-called surface stiffness (or surface rigidity):

$$\tilde{\alpha} = \alpha + \frac{\partial^2 \alpha}{\partial \phi^2}. \quad (2.2.7)$$

For small angles $\phi \ll 1$ on the smooth surface:

$$\tilde{\alpha} = \alpha_0 + \left(\frac{\beta}{d} + 6\gamma \right) |\phi| + \gamma |\phi|^3. \quad (2.2.8)$$

From (2.2.8) we see that $\tilde{\alpha}$ is different from α with respect to the surface anisotropy $\frac{\partial^2 \alpha}{\partial \phi^2}$. For small β , the surface rigidity $\tilde{\alpha}$ is governed by the coefficient γ (by the interaction energy between the steps).

If vice versa β is finite and γ is small then $\tilde{\alpha}$ is governed by β on the smooth surfaces.

For the rough surfaces with only rounded parts it is difficult to define $\tilde{\alpha}$ via the angles ϕ and usually another definition is used:

$$\tilde{\alpha}_{\mu\nu} = \alpha \delta_{\mu\nu} + \frac{\partial^2 \alpha}{\partial \varsigma_\mu \partial \varsigma_\nu}, \quad (2.2.9)$$

where $\varsigma_\mu = \nabla_\mu \varsigma$ is a gradient of the displacement of the surface ς from the initial point. Note that precisely this quantity enters into the spectrum of melting-crystallization waves on rough surfaces (see the next chapter).

Correspondingly we can also express T_R via the surface rigidity $\tilde{\alpha}(T_R)$ in Nozieres theory. Namely according to the universal roughening relation (see Fisher and Weeks [68] and Jayprakash et al. [69]):

$$k_B T_R = \frac{2\tilde{\alpha}(T_R)}{\pi} d^2, \quad (2.2.10)$$

where $\tilde{\alpha} d^2$ is a surface rigidity calculated on one atom for $T = T_R$. Note that the estimates (2.2.5) and (2.2.10) for T_R can be obtained also from the minimization of the Free-energy of the step:

$$\Delta F = \Delta E - T_R \Delta S = 0, \quad (2.2.11)$$

where $\Delta E \sim \beta d$ is an increase of the energy due to the creation of a step at $T = T_R$ and ΔS is a configurational entropy connected with different “charges” of the steps which are situated above or below the averaged surface position. Note also that the exact value of T_R and the behavior of β for $T < T_R$ in Nozieres approach can be extracted from the renorm-group (RG) equations. The renorm-group equations are explicitly derived in [39] and we will not present them here. We just mention that

close to T_R on the smooth side of the transition ($T \leq T_R$) the step-energy β diverges according to the law:

$$\beta(T) \sim \exp \left\{ -\frac{\pi/2 \cdot \text{const}}{\sqrt{1 - T/T_R}} \right\}. \quad (2.2.12)$$

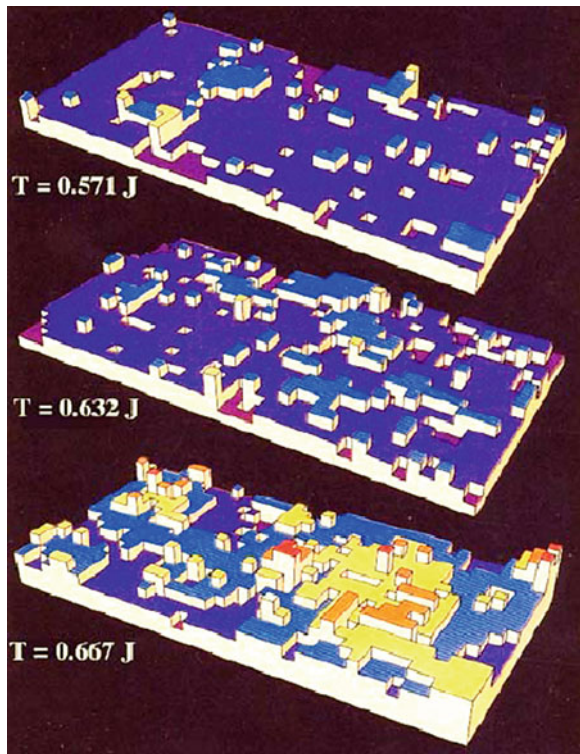
Correspondingly the correlation length $\varsigma(T)$, which enters as a scale in RG-equations, is also exponentially divergent near T_R :

$\varsigma(T) \sim \frac{k_B T_R}{\pi \beta(T)} \rightarrow \infty$ signaling the formation of the macroscopically large step or a flat terrace of the infinite size $\varsigma(T)$. Finally for $T \leq T_R$ the surface rigidity $\tilde{\alpha}(T) \sim \tilde{\alpha}(T_R) \left(1 - \sqrt{1 - T/T_R}\right)$ does not show a critical behavior. Note that the theory of Nozieres considers the periodic pinning surface potential $V(z) = V \cos(2\pi z/d)$ where $z(x)$ is the local height of the surface at the point x . Effectively his RG-approach is based on the Hamiltonian $H = \iint d^2 \vec{r} \left[\frac{1}{2} \tilde{\alpha} (\nabla z)^2 + V \cos \frac{2\pi z}{d} \right]$ and is equivalent to the solution of the sine-Gordon equation $\tilde{\alpha} \frac{d^2 z}{dx^2} + \frac{2\pi}{d} V \sin \left(\frac{2\pi z}{d} \right) = 0$ in the weak coupling limit $V/\tilde{\alpha} \ll 1$. Close to T_R it predicts the formation of the macroscopic step with atomic height given by the expression: $z(x) = \frac{2d}{\pi} \arctg \left(\exp \frac{x}{\varsigma(T)} \right)$, where $\varsigma(T)$ is the coherence length. Note that the limiting values of the height are given by $z(x = -\infty) = 0$ and $z(x = +\infty) = d$ for this solution. Thus, Nozieres theory effectively starts from atomically smooth side and describes the temperature evolution of the system towards the transition to atomically rough state.

It is interesting to compare the analytical renorm-group approach of Nozieres with the results of the numerical simulations by Leamy et al. (see [70] and Fig. 2.10). The roughening transition in these simulations $T_R \sim \beta d \cdot 0.632$ corresponds, crudely speaking, to the estimate (2.2.11) $T_R \sim \frac{\beta d}{\Delta S}$ with configurational entropy ΔS approximately equals to $\ln 3$ (see [40]. From the other hand numerical simulations (see Fig. 2.10) are in favor of an important role of kinks or adatoms for the understanding of the roughening transition. Note that delocalized kinks or adatoms serve as a cornerstone of Andreev, Parshin scenario of quantum roughening, while in Nozieres theory (which is a more classical one) only linear surface defects—the steps are introduced and deeply investigated. We have a feeling that a complete quantum picture of roughening transition is far from understanding and requires the consideration of 2D gas of steps and kinks on equal grounds. In this context we should mention the $T = 0$ predictions of the exactly solvable quantum models considered by Iordansky and Korshunov [44].

From the experimental side the different groups (Balibar et al. [71], Andreeva et al. [72, 73], Babkin et al. [74], Wolf et al. [75], Rolley et al. [76–78]) measured the angular dependence of the surface rigidity $\tilde{\alpha}(\varphi)$ and linear contribution to $\tilde{\alpha}(\varphi)$ for small φ (corresponding to the step formation). The experiments were performed at different temperatures and lead to the observation of the roughening

Fig. 2.10 Numerical simulations by Leamy et al. [70] illustrating the basic physics of a roughening transition. The crystal has a simple cubic lattice and each atom is represented by a cube. At low temperature, there are very few defects such as adatoms, surface vacancies, steps and terraces. As temperature increases, steps proliferate and the crystal surface loses reference to the lattice. The temperature is expressed as a function of the bond energy J . The roughening transition occurs at $T_R \sim 0.632 J d^2$ (from Leamy et al. [70], where $J \sim \beta/d$ is the step energy per unit length)



transitions for three particular atomically smooth surfaces at the temperatures $T_{R1} = 1.28$ K, $T_{R2} = 0.9$ K and $T_{R3} = 0.35$ K correspondingly. They also show the increase of the faceted area fraction (in comparison with the total area of the crystal surface) when we decrease the temperature. In the same time many surfaces remain atomically rough till low temperatures. In particular for some crystallographic directions (which are described by large Miller indices and can be obtained by tilting on a small angle of the main crystallographic surface) there are families of the so-called vicinal surfaces staying in atomically rough state till very low temperatures. These temperatures are less than typical phonon temperatures $T_{ph} \sim (0.4 \div 0.5)$ K in liquid He-II.

Thus the very interesting question whether we can have atomically (or quantum) rough surface precisely at $T = 0$ is still a subject of a debate today.

In the next chapter we will detaily consider the hydrodynamic aspect of this discussion, namely a spectrum of weakly damped melting-crystallization waves. The existence of the weakly damped low frequency branch of the spectrum and its hydrodynamic derivation based on the condition of thermodynamic equilibrium serve as a good proof of a mobile character of many phase-interfaces till relatively low temperatures. Experiments of Keshishev et al. and Balibar et al. on melting-crystallization waves were done until the temperature as low as 0.25 K, which is a

direct proof that even at these temperatures many surfaces are still atomically rough. Moreover the melting-crystallization waves were observed on the surface of solid ^3He even at much lower temperatures in Helsinki [40, 79]. In the last case, however, the spectrum was not detailly measured. So we cannot say a priori whether these waves are linear melting-crystallization waves predicted by Andreev, Parshin for rough surfaces or nonlinear waves (which exist even on smooth surface) predicted recently by Gusev and Parshin [67].

Concluding this chapter let us emphasize again that in the first part of it we provide an introduction to the concept of quantum crystals and to the interesting problem of possible supersolidity in them. In the second part of this chapter we started to discuss the interesting surface physics on the phase interface between quantum crystals and quantum liquids. We provided an introduction to the problem of roughening transition on the crystal surfaces of solid ^4He and briefly considered the spectrum of melting-crystallization waves on rough surface as well as Rayleigh waves, which exist both on rough and smooth surfaces. The next chapter will be devoted to the construction of quantum hydrodynamics on the mobile rough surfaces at low temperatures.

References

1. Kittel, C.: Quantum Theory of Solids. Wiley, New York (1963)
2. Kittel, C.: Introduction to Solid State Physics, 6th edn. Wiley, New York (1986)
3. de Boer, J.: *Physica* **14**, 139 (1948)
4. Andreev, A.F., Lifshitz, I.M.: *JETP* **29**, 1107 (1969)
5. Landau, L.D., Lifshitz, E.M.: Elasticity Theory. Pergamon, Oxford (1959)
6. Burns, C.A., Goodkind, J.M.: *J. Low Temp. Phys.* **95**, 695 (1994)
7. Gardner, W.R., Hoffer, J.K., Phillips, N.E.: *Phys. Rev. A* **7**, 1029 (1973)
8. Kim, E., Chan, M.H.W.: *Science* **305**, 1941 (2004)
9. Kim, E., Chan, M.H.W.: *Nature* **427**, 225 (2004)
10. Kim, E., Chan, M.H.W.: *J. Low Temp. Phys.* **138**, 859 (2005)
11. Kim, E., Chan, M.H.W.: *Phys. Rev. Lett.* **97**, 115302 (2006)
12. Kim, E., Chan, M.H.W.: The Plenary Talk at LT-24 Conference. Orlando, USA (2005)
13. Clark, A.C., Lin, X., West, J. Chan, M.H.W.: The Plenary Talk on the Conference on Quantum Fluids and Solids (QFS2007), Kazan, Russian Federation (2007)
14. Andronikashvili, E.L.: *JETP* **18**, 424 (1948)
15. Leggett, A.J.: *Phys. Rev. Lett.* **25**, 1543 (1970)
16. Matsuda, H., Tsuneto, T.: *Suppl. Progr. Theor. Phys.* **46**, 411 (1970)
17. Chester, G.V.: *Phys. Rev. A* **2**, 256 (1970)
18. Reatto, L.: *Phys. Rev.* **183**, 334–338 (1969)
19. Penrose, O., Onsager, L.: *Phys. Rev.* **104**, 576 (1956)
20. Yang, S.N.: *Rev. Mod. Phys.* **34**, 694 (1962)
21. Penrose, O.: *Phil. Mag.* **42**, 1373 (1951)
22. Anderson, P.W., Brinkman, W.F., Huse, D.A.: *Science* **310**, 1164–1166 (2005)
23. Anderson, P.W.: arXiv:cond-mat/0603726 (2006)
24. Balatsky, A.V., Abrahams, E.: *J. Supercond. Novel Magn.* **19**, 395 (2006)
25. Nussinov, Z., Balatsky, A.V., Graf, M.J., Trugman, S.A.: *Phys. Rev. B* **76**, 014530 (2007)
26. Balatsky, A.V., Graf, M.J., Nussinov, Z., Trugman, S.A.: *Phys. Rev. B* **75**, 094201 (2007)

27. Pollet, L., Boninsegni, M., Kuklov, A.B., Prokof'ev, N.V., Svistunov, B.V., Troyer, M.: Phys. Rev. Lett. **98**, 135301 (2007)
28. Boninsegni, M., Prokof'ev, N., Svistunov, B.: Phys. Rev. Lett. **96**, 105301 (2006)
29. Capogrosso-Sansone, B., Prokof'ev, N.V., Svistunov, B.V.: Phys. Rev. B **75**, 134302 (2007)
30. Prokof'ev, N., Svistunov, B.: Phys. Rev. Lett. **94**, 155302 (2005)
31. Prokof'ev, N.V.: Adv. Phys. **56**, 301 (2007)
32. Sasaki, S., Ishiguro, R., Caupin, F., Maris, H.J., Balibar, S.: Science **313**, 1098–1100 (2006)
33. Andreev, A.F.: JETP Lett. **85**, 585 (2007)
34. Andreev, A.F.: JETP **108**, 1157 (2009)
35. Andreev, A.F.: JETP Lett. **94**, 129 (2011)
36. Rittner, A.S.C., Reppy, J.D.: Phys. Rev. Lett. **98**, 175302 (2007)
37. Day, J., Beamish, J.: Phys. Rev. Lett. **96**, 105304 (2006). Nature **450**, 853 (2007)
38. Todoshenko, L.A., Alles, H., Parshin, A.Y., Tsepelin, V.: JETP Lett. **85**, 454 (2007)
39. Nozieres, P.: Shape and growth of crystals. In: Godreche, C. (ed.) Solids far from Equilibrium, p. 1. Cambridge University, UK (1991)
40. Balibar, S., Alles, H., Parshin, A.Y.: Rev. Mod. Phys. **77**, 317 (2005)
41. Avron, J.E., Balfour, L.S., Kuper, C.G., Landau, J., Lipson, S.G., Schulman, L.S.: Phys. Rev. Lett. **45**, 814 (1980)
42. Landau, L.D.: The Equilibrium Form of Crystals, in Collected Papers. Pergamon, Oxford (1965)
43. Andreev, A.F.: Defects and surface phenomena in quantum crystals. In: Lifshitz, I.M. (ed.) Quantum Theory of Solids. Mir Publishers, Moscow (1982)
44. Iordanskii, S.V., Korshunov, S.E.: JETP **60**, 528 (1984)
45. Kosterlitz, J.M., Thouless, D.J.: J. Phys. C **6**, 1181 (1973)
46. Berezinskii, V.L.: JETP Lett. **34**, 610 (1972)
47. Andreev, A.F., Parshin, A.Y.: JETP **48**, 763 (1978)
48. Keshishev, K.O., Parshin, A.Y., Babkin, A.V.: JETP Lett. **30**, 56 (1980)
49. Keshishev, K.O., Parshin, A.Y., Babkin, A.V.: JETP **53**, 362 (1981)
50. Kagan, M.Yu.: Superfluid Properties of the Systems with Anisotropic and Inhomogeneous Ordering, Ph.D Thesis. Kapitza Institute (1989)
51. Burns, C.A., Isaak, E.D.: Phys. Rev. B **55**, 5767 (1997)
52. Landau, L.D., Lifshitz, E.M.: Statistical Physics, Part I. Butterworth-Heinemann, Oxford (1999)
53. Lifshitz, E.M., Pitaevskii, L.P.: Statistical Physics, Part II. Pergamon Press, Oxford (1988)
54. Kagan, Y., Maksimov, L.A.: JETP **57**, 459 (1983)
55. Kagan, Y., Maksimov, L.A.: JETP **38**, 307 (1974)
56. Kagan, Y., Maksimov, L.A.: JETP **61**, 583 (1985)
57. Kagan, Y., Klinger, M.I.: Phys. C **7**, 2791 (1974)
58. Landau, L.D., Lifshitz, E.M.: Fluid Mechanics, vol. 6. Butterworth-Heinemann, Oxford (1987). (Course of Theoretical Physics)
59. Kagan, M.Yu.: Superfluidity of quantum crystals: new life of a beautiful idea, in a book commemorated to the 90-th anniversary of Prof. Lifshitz, I.M. (in Russian). In: Baklay, A.C., Volobeyev, A.V., Gredeskul, S.A., et al. (eds.) Kharkov, Syntex LTD (2006)
60. Fraas, B.A., Granfors, P.R., Simmons, R.O.: Phys. Rev. B **39**, 124 (1989)
61. Clark, A.C., Chan, M.H.W.: J. Low Temp. Phys. **138**, 853 (2005)
62. Discussion of Andreev-Lifshitz Theory in Kavli Institute of Theoretical Physics, Santa-Barbara, USA (2006)
63. Kagan, Y.: Private communication to the author, unpublished
64. Castaing, B., Nozieres, P.: J. Phys. **41**, 701 (1980). (France)
65. Marchenko, V.I., Parshin, A.Y.: JETP Lett. **31**, 724 (1980)
66. Chernov, A.V.: Sov. Phys. Uspekhi. **13**, 101 (1970)
67. Gusev, R.B., Parshin, A.Y.: JETP Lett. **85**, 588 (2007)
68. Fisher, D.S., Weeks, J.D.: Phys. Rev. Lett. **50**, 1077 (1983)
69. Jayaprakash, C., Saam, W.F., Teitel, S.: Phys. Rev. Lett. **50**, 2017 (1983)

70. Leamy, H.J., Gilmer, G.H., Jackson, K.A.: In: Blakeley, J.B. (ed.) *Surface Physics of Materials*, p. 121. Academic Press, New York (1975)
71. Balibar, S., Guthmann, C., Rolley, E.: *J. Phys.* **13**, 1475 (1993)
72. Andreeva, O.A., Keshishev, K.O., Osip'yan, S.Y.: *JETP Lett.* **49**, 759 (1989)
73. Keshishev, K.O., Andreeva, O.A.: In: Wyatt, A.F.G., Lauter, H.J. (ed.) *Excitations in Two-Dimensional and Three-Dimensional Quantum Fluids*, p. 387. Plenum, New York (1991)
74. Babkin, A.V., Kopeliovich, D.B., Parshin, A.Y.: *JETP* **62**, 1322 (1985)
75. Wolf, P.E., Gallet, F., Balibar, S., Rolley, E., Nozieres, P.: *J. Phys.* **46**, 1987 (1985). (Paris)
76. Rolley, E., Balibar, S., Graner, F.: *Phys. Rev. E* **49**, 1500–1506 (1994)
77. Rolley, E., Guthmann, C., Chevalier, E., Balibar, S.: *J. Low Temp. Phys.* **99**, 851 (1995)
78. Rolley, E., Chevalier, E., Guthmann, C., Balibar, S.: *Phys. Rev. Lett.* **72**, 872 (1994)
79. Parshin, A.Y.: Private communication to the author, unpublished
80. Lifshitz, E.M., Pitaevskii, L.P.: *Physical Kinetics*. Butterworth-Heinemann, Oxford (1981)
81. Gutzwiller, M.C.: *Phys. Rev. Lett.* **10**, 159 (1963)
82. Bodensohn, J., Nicolai, K., Leiderer, P.: *Zeit. Phys. B: Cond. Mat.* **64**, 55 (1986)
83. Kim, D. Y., Chan, M. H. W.: *Phys. Rev. Lett.*, **109**, 155301 (2012)
84. Schwarzschild, B. M.: *Physics Today*, **65**, 11 (2012)

<http://www.springer.com/978-94-007-6960-1>

Modern trends in Superconductivity and Superfluidity

Kagan, M.Y.

2013, XXIV, 550 p. 216 illus., Softcover

ISBN: 978-94-007-6960-1